Available online at www.sciencedirect.com
ScienceDirect
Scripta Materialia 60 (2009) 627–630
Scripta MATERIALIA
www.elsevier.com/locate/scriptamat

Grain size effect on crack blunting in nanocrystalline materials

I.A. Ovid'ko* and A.G. Sheinerman

Institute of Problems of Mechanical Engineering, Russian Academy of Sciences, Bolshoj 61, Vasil. Ostrov, St Petersburg 199178, Russia

Received 31 October 2008; revised 10 December 2008; accepted 13 December 2008
Available online 25 December 2008

The effect of grain size on the blunting of cracks in nanocrystalline materials is described theoretically. Within our description, lattice dislocations emitted from cracks are stopped at grain boundaries. The stress fields of these dislocations suppress further dislocation emission from cracks in nanomaterials, and the suppression depends on grain size. The dependence of the number of dislocations emitted by a crack on grain size in nanocrystalline Ni is calculated, and characterizes the grain size effect on crack blunting.

Keywords: Nanocrystalline materials; Cracks; Dislocations

Plastic deformation and fracture processes in nanocrystalline metals and ceramics are the subject of rapidly growing research efforts motivated by development of technologies exploiting the outstanding mechanical properties of these materials (e.g., [1–15]). Nanomaterials generally have superior strength and hardness but low tensile ductility characterized by strain-to-failure of 2–3% at room temperature [1–4]. In particular, the specific fracture behavior of nanomaterials manifests itself in the experimental fact that some nanocrystalline metals with a face-centered-cubic (fcc) lattice exhibit a ductile-to-brittle transition with decreasing grain size [16–18]. In contrast, good ductility is always inherent to coarse-grained fcc metals where emission of lattice dislocations from cracks causes effective blunting of cracks and thus suppresses their growth. In the context discussed, in order to understand and control the specific fracture behavior of nanomaterials, it is very important to identify the sensitivity of crack blunting processes to nanocrystallinity. The main aim of this paper is to describe theoretically the grain size effect on the blunting of cracks in nanomaterials. Particular attention will be paid to the role of grain boundaries (GBs) as structural elements that hinder the blunting of cracks in nanomaterials.

Let us consider a model infinite nanocrystalline solid under a remote one-axis tensile loading. The solid is supposed to be elastically isotropic and have the shear modulus G and Poisson ratio v. Let a long, flat crack grow in the solid. If the stress intensity near the crack tip is large enough, the crack induces plastic shear through the emission of a lattice dislocation from the crack tip. Since GBs serve as obstacles to lattice dislocation slip [1–4], we assume that the emitted dislocation is retarded at the neighboring GB. In general, the emission of the first dislocation is followed by the emission of the next dislocations along the same slip plane. These new dislocations slip until they reach their equilibrium positions determined by the balance of the force exerted by the applied shear stress (which promotes dislocation slip) and the force exerted by the previously emitted dislocations (which hinders dislocation slip).

If the grain size of the solid is sufficiently large, the emitted dislocations move far enough from the crack tip and do not significantly hinder the motion of new dislocations until the number of the emitted dislocations becomes large enough. In this case, the dislocation emission along one slip plane can induce significant blunting of the crack tip. Following Refs. [19–21], the significant blunting both stops crack growth and makes the solid ductile. At the same time, in nanomaterials, the emission of even one dislocation and its arrest at the nearest GB hinder the emission of subsequent dislocations along the same plane due to dislocation repulsion. In doing so, the dislocation emission does not induce significant crack blunting. As a corollary, the nanocrystalline solid tends to show a brittle behavior.

Note that the above scenario is realized in the situation where slip of lattice (perfect or partial) dislocations

* Corresponding author. Tel.: +7 812 321 4764; fax: +7 812 321 4771; e-mail addresses: ovidko@def.ipme.ru, shein@def.ipme.ru

1359-6462/$ - see front matter
doi:10.1016/j.scriptamat.2008.12.028

dominates in nanocrystalline materials. In particular, it is the case of room temperature deformation of nanocrystalline and ultrafine-grained metals having grain size d larger than a critical size $d_c \approx 20$ nm [1–4]. In these materials, one expects that emission of lattice dislocations from crack tips is the dominant micromechanism for crack blunting at room temperature. Our view is supported by the experimental "in situ" observation [22] of the dominant role of lattice-dislocation plasticity near crack tips in nanocrystalline Ni with mean grain size $d = 23$ nm. In contrast, GB sliding plays an important or even dominant role in plastic flow in nanocrystalline metals with the finest grains ($d < 20$ nm) at room temperature and nanocrystalline metals and ceramics with widely ranging grain sizes at elevated temperatures [1–4]. In these materials, one expects that both lattice dislocation slip and GB sliding contribute to the blunting of cracks. This view is supported by computer simulations [23] showing that lattice dislocation emission and GB deformation processes contribute approximately 60% and 40%, respectively, to the blunting of a crack in nanocrystalline α-Fe with grain size $d = 9$ nm. In our short paper, for simplicity, we consider the emission of only lattice dislocations from cracks. In doing so, our model effectively describes the crack blunting in nanocrystalline and ultrafine-grained metals with grain sizes $d > 20$ nm at room temperature, and approximately describes the crack blunting in other nanomaterials.

Let us calculate the number N of dislocations emitted from a crack along one slip plane as a function of grain size d. For simplicity, we consider the case of pure mode I loading, characterized by the stress intensity factor K_I created by an applied tensile load. We focus on the case where the crack length is much larger than d. In this case, the crack can be modeled as a semi-infinite one. Let the crack lie along the half-plane ($y = 0$, $x < 0$) in the coordinate system (x, y) shown in Figure 1, and let several dislocations be emitted from the crack tip (Fig. 1) under the action of the applied stress concentrated at the tip. For simplicity, we focus on the situation where the dislocations are of edge character and their Burgers vectors lie along the slip plane that makes an angle θ with the x-axis (Fig. 1).

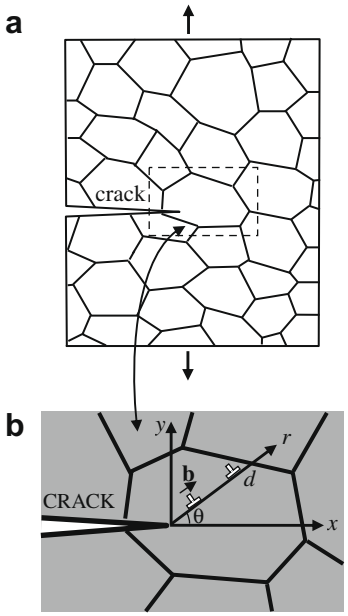

Figure 1. Crack in a deformed nanocrystalline solid. (a) General view. (b) The magnified inset highlights lattice dislocation emission from a crack tip.

The first (leading) dislocation stops at a GB at a distance d from the crack tip. The equilibrium positions of the other dislocations are calculated from the force balance equations $F_r^k = 0$, where $k = 2, ..., N$; and F_r^k is the projection of the force $\mathbf{F}^k$ on the r-axis (see Fig. 1). The total force F_r^k acting on the kth dislocation can be rewritten in terms of the effective stress $\sigma_{r\theta}^e(r_k, \theta)$ acting on the kth dislocation (where r_k is the distance from the kth dislocation to the crack tip) and defined as: $F_r^k = b\sigma_{r\theta}^e(r_k, \theta)$. This effective stress can be presented as:

$$\sigma_{r\theta}^e(r_k, \theta) = \sigma_{r\theta}^{K_I}(r_k, \theta) + \sigma_{r\theta}^{im}(r_k, \theta) + \sum_{\substack{j=1,\\ j\neq k}}^{N} \sigma_{r\theta}(r_k, r_j, \theta), \quad (1)$$

where the stress $\sigma_{r\theta}^{K_I}(r_k, \theta)$ is created by the applied load near the crack tip and corresponds to the force exerted by the applied load on the kth dislocation; the image stress $\sigma_{r\theta}^{im}(r_k, \theta)$ is associated with the presence of the crack free surface and corresponds to the image force induced by the crack; and the stress $\sigma_{r\theta}(r_k, r_j, \theta)$ is created by the jth dislocation at the point (r_k, θ) and corresponds to the force exerted on the kth dislocation by the jth dislocation.

To be emitted from the crack tip, all dislocations have to overcome the crack tip attraction zone associated with the presence of the image stress $\sigma_{r\theta}^{im}(r_k, \theta)$. Following the Rice–Thompson criterion [19], we assume that the emission of the first dislocation occurs if this dislocation is repelled from the crack tip whenever the distance from the dislocation to the crack tip exceeds the dislocation core radius r_0. Then the critical condition for the emission of the first dislocation is:

$$\sigma_{r\theta}^{K_I}(r_1, \theta) + \sigma_{r\theta}^{im}(r_1, \theta)|_{r=r_0} > 0. \quad (2)$$

If the first dislocation moves far enough from the crack tip, it only slightly increases the crack tip attraction zone for the second emitted dislocation. In this case, the second dislocation can overcome this attraction zone and is then repelled from the crack tip until it reaches its equilibrium position. At the same time, if the first emitted dislocation stops at a GB located very close to the crack tip, it can completely eliminate the region where the following dislocation is repelled from the crack tip, making the emission of the next dislocation impossible.

For definiteness, in the following, we consider only necessary conditions for dislocation emission and suppose that dislocation emission can be possible even if the width of the crack tip attraction zone exceeds the dislocation core radius. We assume that the emission of the $(N+1)$th dislocation $(N = 1, 2, \ldots)$ can occur if there is a region within the interval $0 < r < d$ where this dislocation is repelled from the crack tip. In this region, the following inequality should be valid:

$$\sigma_{r\theta}^{K_I}(r_{N+1},\theta)+\sigma_{r\theta}^{im}(r_{N+1},\theta)+\sum_{j=1}^{N}\sigma_{r\theta}(r_{N+1},r_j,\theta)>0. \quad (3)$$

Note that formula (3) gives only necessary, but not sufficient, condition for the dislocation emission. Therefore, the real conditions for the dislocation emission are stricter than those described by formula (3).

Let us calculate the stresses $\sigma_{r\theta}^{K_I}(r_k,\theta)$, $\sigma_{r\theta}^{im}(r_k,\theta)$ and $\sigma_{r\theta}(r_k,r_j,\theta)$ appearing in formulas (1)–(3). The stress $\sigma_{r\theta}^{K_I}(r_k,\theta)$ that corresponds to the force of the interaction between the kth dislocation and the applied stress near the crack tip is given by [24]:

$$\sigma_{r\theta}^{K_I}(r_k,\theta)=\frac{K_I\sin\theta\cos(\theta/2)}{2\sqrt{2\pi r_k}}. \quad (4)$$

The image stress $\sigma_{r\theta}^{im}(r_k,\theta)$ that corresponds to the force of the interaction between the kth dislocation and the crack free surface is given as [24]:

$$\sigma_{r\theta}^{im}(r_k,\theta)=-\frac{Gb}{4\pi(1-\nu)r_k}, \quad (5)$$

where b is the magnitude of the dislocation Burgers vector.

The stress $\sigma_{r\theta}(r,r_j,\theta)$ created by the jth dislocation at the point (r,θ) is expressed in terms of the Cartesian stress field components σ_{xx}, σ_{yy} and σ_{xy} as:

$$\sigma_{r\theta}=\left(\sigma_{yy}-\sigma_{xx}\right)\sin\theta\cos\theta+\sigma_{xy}\cos(2\theta). \quad (6)$$

The stresses σ_{xx}, σ_{yy} and σ_{xy} follow Ref. [24] as $\sigma_{yy}=\mathrm{Re}\,g$, $\sigma_{xy}=-\mathrm{Im}\,g$, $\sigma_{xx}=\mathrm{Re}[4\varphi'-g]$, where $g=\varphi'+\bar{\omega}'+(z-\bar{z})\bar{\varphi}''$, φ and ω are the complex functions of the complex variable $z=x+iy$ and $i=\sqrt{-1}$. The quantities φ' and $\bar{\omega}'$ for an edge dislocation located at the point $z_j=x_j+iy_j$ follow from Ref. [24] as:

$$\varphi'=A\left(\frac{1}{z-z_j}\left(\sqrt{\frac{z_j}{z}}+1\right)+\frac{1}{z-\bar{z}_j}\left(\sqrt{\frac{\bar{z}_j}{z}}-1\right)\right)+\frac{\bar{A}(z_j-\bar{z}_j)}{2(z-\bar{z}_j)^2}\left(\sqrt{\frac{\bar{z}_j}{z}}+\sqrt{\frac{z}{\bar{z}_j}}-2\right), \quad (7)$$

$$\bar{\omega}'=A\left(\frac{1}{\bar{z}-z_j}\left(\sqrt{\frac{z_j}{\bar{z}}}-1\right)+\frac{1}{\bar{z}-\bar{z}_j}\left(\sqrt{\frac{\bar{z}_j}{\bar{z}}}+1\right)\right)+\frac{\bar{A}(z_j-\bar{z}_j)}{2(\bar{z}-\bar{z}_j)^2}\left(\sqrt{\frac{\bar{z}_j}{\bar{z}}}+\sqrt{\frac{\bar{z}}{\bar{z}_j}}+2\right), \quad (8)$$

where $A=G(b_x+ib_y)/[8\pi i(1-\nu)]$. In the case shown in Figure 1, we have: $b_x=b\cos\theta$, $b_y=b\sin\theta$, and $z_j=r_je^{i\theta}$.

Formula (1) and Eqs. (4)–(8) allow the total stresses $\sigma_{r\theta}^{e}(r_k,\theta)$ acting on dislocations to be calculated. To calculate the number N of lattice dislocations that can be emitted along the same slip plane, we use the following calculation procedure. First, we verify validity of criterion (2) for emission of the first dislocation. If this criterion is valid, we place the first dislocation at the distance d from the crack tip and verify validity of criterion (3) for the emission of the second dislocation. If this criterion is valid for the second dislocation, we calculate its equilibrium position and check validity of criterion (3) for emission of the third dislocation, and so on. The procedure is carried out for all the new emitted dislocations and ends when criterion (3) for the emission of a new dislocation stops to be valid.

With this calculation procedure, we have calculated the number N of lattice dislocations emitted along the same plane as a function of grain size d, for nanocrystalline Ni (Fig. 2). For definiteness, we put $\theta=\pi/3$ and $K_I=K_{IC}$, where $K_{IC}=\sqrt{4G\gamma/(1-\nu)}$ is the brittle fracture toughness and γ is the specific surface energy. We have also used the following typical values of parameters of Ni: $G=73$ GPa, $\nu=0.34$, $\gamma=1.725$ J m^{-2} and $b=0.25$ nm. Figure 2 shows that N significantly decreases with a decrease in grain size d. In particular, $N=10$ at $d=200$ nm, and $N=4$ at $d=30$ nm. This means that, for small grain sizes, dislocation emission along one slip plane cannot lead to a significant crack blunting. In this case, the crack can easily grow, though its growth rate is lowered by plastic deformation near crack tip. Therefore, when the grain size of a nanocrystalline solid is lower than a critical value, the solid shows a ductile-to-brittle transition. The fracture behavior of such a solid undergoing the ductile-to-brittle transition is characterized by a slow crack growth, which can eventually (but not immediately) result in the complete fracture of the solid. This conclusion is supported by experiments [16,17] showing that a nanocrystalline Ni–15% Fe specimen with the grain size $d=9$ nm fractures due to brittle crack propagation but, at the same time, demonstrates a high enough strain-to-failure of 8%. Generally speaking, in the case of $d<20$ nm, one should take into account GB deformation processes that contribute to the blunting of cracks and increase strain-to-failure. At the same time, our preliminary analysis definitely shows that accounting for GB deformation processes does not change the key conclusions of this paper.

Thus, we have theoretically revealed that blunting of cracks through lattice dislocation emission is highly sensitive to the grain size in nanocrystalline and ultrafine-grained materials at room temperature. In particular, grain boundaries effectively suppress both the dislocation emission from crack tips and thereby the blunting of cracks in nanocrystalline metals with comparatively small grains. As a corollary, when the grain size of a nanocrystalline solid decreases, the solid tends to show a brittle behavior. This theoretical conclusion is in a good agreement with the experimentally detected fact [16–18] that some nanocrystalline fcc metals exhibit a ductile-to-brittle transition with decreasing grain size.

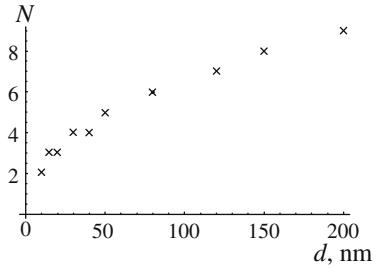

Figure 2. The maximum number N of edge dislocations (that can be emitted from the crack tip along one slip plane) as a function of grain size d in nanocrystalline Ni.

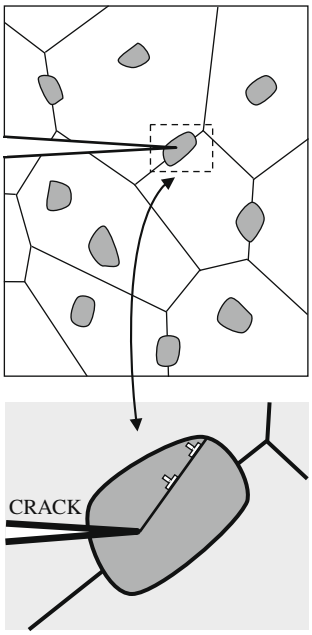

Figure 3. A crack grows in a deformed ceramic–matrix nanocomposite containing metallic nanoinclusions (gray regions) in grain interiors and at grain boundaries. The magnified inset highlights lattice dislocation emission from the crack tip penetrating a metallic nanoinclusion.

Finally, note that our theoretical results are interesting for understanding the mechanisms of ductile phase toughening [25] in ceramic nanocomposites consisting of a ceramic matrix and ductile metallic nanoinclusions (Fig. 3). The toughening is realized through plastic deformation of metallic nanoinclusions, which relieves high local stresses near a crack tip and thus hampers crack growth. Plastic deformation of metallic nanoinclusions occurs in part via emission of lattice dislocations from the crack tip penetrating a metallic nanoinclusion (Fig. 3). In these circumstances, with the results of this paper, one expects that toughness of nanoceramics with metallic nanoinclusions is highly sensitive to sizes of nanoinclusions, because of the theoretically revealed grain size effect on blunting of cracks. More precisely, the ductile phase toughening is enhanced in ceramic nanocomposites when the typical size of metallic nanoinclusions increases.

The work was supported, in part, by the Russian Foundation of Basic Research (Grant 08-01-00225-a), the Office of Naval Research (Grant N00014-08-1-0405), the National Science Foundation (Grant CMMI #0700272), and the Russian Federal Agency of Science and Innovations (Grant MK-1702.2008.1).

[1] D. Wolf, V. Yamakov, S.R. Phillpot, A.K. Mukherjee, H. Gleiter, Acta Mater. 53 (2005) 1.
[2] M. Dao, L. Lu, R.J. Asaro, J.T.M. De Hosson, E. Ma, Acta Mater. 55 (2007) 4041.
[3] C.C. Koch, J. Mater. Sci. 42 (2007) 1403.
[4] C.C. Koch, I.A. Ovid'ko, S. Seal, S. Veprek, Structural Nanocrystalline Materials: Fundamentals and Applications, Cambridge University Press, Cambridge, 2007.
[5] R.W. Siegel, S.K. Chang, B.J. Ash, J. Stone, P.M. Ajayan, R.W. Doremus, L.S. Schadler, Scripta Mater. 44 (2001) 2061.
[6] G.-D. Zhan, J.D. Kuntz, J. Wan, J. Garay, A.K. Mukherjee, Scripta Mater. 47 (2002) 737.
[7] M. Jin, A.M. Minor, E.A. Stach, J.W. Morris Jr., Acta Mater. 52 (2004) 5381.
[8] W.A. Soer, J.Th.M. De Hosson, A.M. Minor, J.W. Morris Jr., E.A. Stach, Acta Mater. 52 (2004) 5783.
[9] R.S. Kottada, A.H. Chokshi, Scripta Mater. 53 (2005) 887.
[10] J.T.M. De Hosson, W.A. Soer, A.M. Minor, Z. Shan, E.A. Stach, S.A. Syed Asif, O.L. Warren, J. Mater. Sci. 41 (2006) 7704.
[11] K.M. Youssef, R.O. Scattergood, K.L. Murty, C.C. Koch, Scripta Mater. 54 (2006) 251.
[12] P.L. Gai, K. Zhang, J. Weertman, Scripta Mater. 56 (2007) 25.
[13] W. Blum, Y.J. Li, Scripta Mater. 56 (2007) 429.
[14] I.A. Ovid'ko, J. Mater. Sci. 42 (2007) 1694.
[15] J. Lian, J.E. Garay, J. Wang, Scripta Mater. 56 (2007) 1095.
[16] H. Li, F. Ebrahimi, Appl. Phys. Lett. 84 (2004) 4307.
[17] H. Li, F. Ebrahimi, Adv. Mater. 17 (2005) 1969.
[18] F. Ebrahimi, A.J. Liscano, D. Kong, Q. Zhai, H. Li, Rev. Adv. Mater. Sci. 13 (2006) 33.
[19] J.R. Rice, R.M. Thompson, Phil. Mag. 29 (1974) 73.
[20] J.R. Rice, J. Mech. Phys. Sol. 40 (1992) 239.
[21] G.E. Beltz, D.M. Lipkin, L.L. Fischer, Phys. Rev. Lett. 82 (1999) 4468.
[22] K.S. Kumar, S. Suresh, M.F. Chisholm, J.A. Norton, P. Wang, Acta Mater. 51 (2003) 387.
[23] A. Latapie, D. Farkas, Phys. Rev. B 69 (2004) 134110.
[24] I.-H. Lin, R. Thompson, Acta Metall. 34 (1986) 187.
[25] G.-D. Zhan, J.D. Kuntz, A.K. Mukherjee, MRS Bull. 29 (2004) 22.